Infection and Drug Resistance

Dovepress
Taylor & Francis Group

Open Access Full Text Article

ORIGINAL RESEARCH

Comparative Genomic Analysis of *Pseudomonas aeruginosa* Isolates from Community-Acquired and Hospital-Acquired Pneumonia

Feifei Yang[1,*], Shukun Chai[2,*], Li Yan[3,*], Yukun He[1], Xinqian Ma[1], Lixiao Shen[2], Shuhui Gao[3], Yatao Guo[1,4], Zhao Zhang[1,4], Wentao Ni[1], Jing Bao[1], Zhancheng Gao[1]

[1]Department of Respiratory and Critical Care Medicine, Peking University People's Hospital, Beijing, People's Republic of China; [2]Department of Respiratory Medicine, Shijiazhuang People's Hospital, Shijiazhuang, Hebei, People's Republic of China; [3]Department of Respiratory Medicine, Hebei General Hospital, Shijiazhuang, Hebei, People's Republic of China; [4]Department of Respiratory and Critical Care Medicine, The First Affiliated Hospital of Zhengzhou University, Zhengzhou, Henan, People's Republic of China

*These authors contributed equally to this work

Correspondence: Jing Bao; Zhancheng Gao, Department of Respiratory and Critical Care Medicine, Peking University People's Hospital, Beijing, 100044, People's Republic of China, Email levelooo@bjmu.edu.cn; zcgao@bjmu.edu.cn

Purpose: To characterize the genomic features of *Pseudomonas aeruginosa* isolates causing community-acquired pneumonia (CAP) and compare them with hospital-acquired pneumonia (HAP) genomes to identify setting-associated genetic determinants.

Patients and Methods: Three CAP isolates collected in China underwent antimicrobial susceptibility testing and whole-genome sequencing. Comparative genomic analyses were performed against 84 complete HAP-associated genomes retrieved from NCBI RefSeq (accessed in December 2023), including core genome SNP phylogeny, profiling of antimicrobial resistance (AMR) determinants, virulence genes, and pangenome analysis to identify CAP-specific genes.

Results: The three CAP cases presented with severe pneumonia (including septic shock), with one fatality; however, all CAP isolates remained susceptible to the most commonly used antipseudomonal agents. CAP genomes were 6.5–7.1 Mb (GC 65.76–66.41%) and contained 5908–6633 predicted coding sequences. Core-SNP phylogeny showed clustering of the three CAP isolates. Compared with HAP genomes, CAP isolates harbored fewer acquired AMR genes and fewer resistance-associated mutations. Virulence profiling identified a subset of virulence genes absent from all CAP genomes (n = 40), largely annotated as immune modulation and including loci consistent with highly variable surface polysaccharide regions, together with several genes annotated to biofilm-related functions and effector delivery systems. Major type III secretion system effector profiles differed across CAP isolates (*exoU* in one isolate; *exoS* in two). Pangenome analysis identified 10,225 gene families, and 157 genes were specific to the CAP isolates, most encoding hypothetical proteins, with a subset related to lipid transport and metabolism, including fatty acid uptake and functions associated with β-oxidation. Given the limited number of CAP isolates, comparisons between groups are descriptive.

Conclusion: CAP-associated *P. aeruginosa* showed a distinct comparative genomic profile with reduced AMR determinant burden and a distinct virulence gene repertoire despite severe clinical presentation. CAP-specific genes, including those linked to lipid metabolism, may contribute to niche adaptation and warrant functional validation.

Keywords: *Pseudomonas aeruginosa*, community-acquired pneumonia, hospital-acquired pneumonia, comparative genomics, virulence, antimicrobial resistance

Introduction

Pseudomonas aeruginosa is a gram-negative opportunistic pathogen that plays a central role in nosocomial infections, particularly in immunocompromised individuals and those with structural lung diseases, such as cystic fibrosis.[1] *P. aeruginosa* is primarily recognized as a hospital-associated pathogen, but it has also been reported as a rare cause of community-acquired pneumonia (CAP). When it causes CAP, the clinical outcomes are often severe, with high

https://doi.org/10.2147/IDR.S566637
Received: 21 October 2025
Accepted: 4 February 2026
Published: 13 February 2026

morbidity and mortality.[2] Although relatively rare, CAP caused by *P. aeruginosa* has been increasingly reported. Nevertheless, our understanding of the genetic factors underlying the pathogenicity of CAP remains limited.

P. aeruginosa genomes range in size from 5.5 to 7.0 Mb, with a GC content of 65–67% and 79 regions of extensive genome plasticity.[3] This considerable genome size and plasticity enhance the bacterium's adaptability during prolonged infections.[4] Additionally, comparative genomic analysis reveals that the *P. aeruginosa* genome is a mosaic of conserved sequences and accessory elements, which may encode traits for niche-specific adaptation.[5] However, most studies have focused on strains isolated from eye and cystic fibrosis infections.[6,7] Investigating the genomic and environmental factors that contribute to the ability of *P. aeruginosa* to cause CAP is crucial for improving early detection and treatment strategies.

P. aeruginosa can develop resistance and virulence by selecting genomic mutations, exchanging transferable resistance or virulence determinants.[8] Numerous chromosomal mutations and acquired antimicrobial resistance (AMR) genes have been reported to contribute to the improved antibiotic resistance shown by *P. aeruginosa*.[9,10] The expression of these resistance determinants poses a challenge in treating infections caused by *P. aeruginosa*, especially respiratory infections. Furthermore, *P. aeruginosa* harbors a diverse array of virulence factors, including type III secretion system (T3SS), quorum sensing, biofilm formation, secreted siderophores, proteases, and exopolysaccharides,[11] all of which contribute to its potential to cause severe CAP.

In this study, we analyzed three clinical cases of *P. aeruginosa* CAP and performed comparative genomic analyses of the corresponding isolates in comparison with *P. aeruginosa* genomes associated with HAP. Our objective was to characterize infection-setting–associated differences between CAP and HAP isolates in antimicrobial resistance determinants and virulence gene content, and to identify CAP accessory genes that may contribute to niche adaptation and pathogenic potential. We therefore applied a comparative genomics framework comprising core-genome phylogeny, systematic AMR and virulence profiling, and pangenome analysis to identify CAP-specific genes.

Materials and Methods

Bacterial Sample Collection and Clinical Data Collection

Three non-duplicate *P. aeruginosa* isolates were collected between January 2016 and December 2022 from sputum or bronchoalveolar lavage fluid (BALF) specimens of patients diagnosed with CAP at Peking University People's Hospital, Hebei General Hospital, and Shijiazhuang People's Hospital in China. CAP was defined as pneumonia with symptom onset in the community or within 48 h of hospital admission, without hospitalization in the preceding 90 days. Key clinical, laboratory, and imaging variables were abstracted from medical records to describe case presentation and clinical course.

Species Identification and Antimicrobial Susceptibility Testing

The three CAP *P. aeruginosa* isolates were cultured on Columbia blood agar supplemented with 5% sheep blood at 37°C for 18–24 h. Species identification was confirmed by matrix-assisted laser desorption/ionization time-of-flight mass spectrometry (MALDI-TOF MS; bioMérieux, France) according to the manufacturer's instructions. Briefly, a single colony was applied to the target plate, spectra were generated by laser desorption/ionization, and the resulting mass spectral fingerprint was matched against the reference database for species assignment. Antimicrobial susceptibility testing was performed by broth microdilution for each antimicrobial agent. *P. aeruginosa* ATCC 27853 served as the quality-control strain. Results were interpreted according to the Clinical and Laboratory Standards Institute (CLSI) M100 guideline.

DNA Extraction and Sequencing

The three CAP *P. aeruginosa* isolates were grown as overnight cultures in LB broth at 37°C with shaking for genomic DNA preparation. Genomic DNA was extracted using the DNeasy Blood & Tissue Kit (Qiagen, Hilden, Germany) according to the manufacturer's instructions. DNA integrity was assessed by 1% agarose gel electrophoresis. DNA yield and purity were measured using a NanoDrop™ 2000 spectrophotometer (Thermo Fisher Scientific, USA) and a TBS-380 fluorometer (Turner BioSystems Inc., Sunnyvale, CA). Only high-quality DNA (OD260/280 = 1.8–2.0; total DNA ≥1 μg) was used for sequencing. Long-read sequencing was performed on the PacBio *RS* II platform, and SMRTbell libraries were prepared

with 20 kb inserts. Subreads shorter than 500 bp were removed prior to downstream processing. De novo assembly was performed using Canu v2.2,[12] and the assembled genomes were annotated using Prokka v1.14.6.[13]

Comparative Genomics and Gene Identification

For comparative analyses, 84 complete *P. aeruginosa* genomes annotated as HAP isolates were retrieved from NCBI RefSeq (accessed in December 2023) (Supplementary Table 1). tRNA genes were identified using tRNAscan-SE v2.0.9, and rRNA genes were identified using rRNAmmer v1.2. Acquired antimicrobial resistance and virulence genes were identified using ABRicate v1.0.1 with the CARD and Virulence Factor Database (VFDB) databases. Default thresholds were applied (≥90% identity and ≥80% coverage).[14,15] Chromosomal resistance-associated variants in *P. aeruginosa* were annotated from single nucleotide polymorphisms (SNPs) and insertions/deletions (InDels) using SnpEff v5.0. Genes involved in mutational resistance (PAO1 as the reference) were selected and analyzed based on previous studies.[16]

Statistical Analysis

Given the limited number of CAP isolates (n = 3), analyses were designed to be descriptive and hypothesis generating rather than inferential. Formal hypothesis testing was therefore not performed. Differences between groups in AMR determinants, resistance associated variants, virulence gene presence or absence, and pangenome features are presented descriptively using counts, proportions, and presence or absence visualizations.

Phylogenetic Analysis

Multilocus sequence typing (MLST) was performed using the PubMLST *Pseudomonas aeruginosa* database (https://pubmlst.org/paeruginosa). Assembled genome sequences were queried against the PubMLST MLST scheme to determine the allelic profiles and assign sequence types (STs). Isolates with allele profiles not matching any existing ST in PubMLST at the time of analysis were considered putative novel STs. SNP calling was performed using Snippy v4.6.0 with *P. aeruginosa* PAO1 (GenBank accession No. NC_002516.2) as the reference genome. Recombination in the core SNP alignment was filtered using Gubbins v3.2.1. A maximum-likelihood phylogeny was inferred using FastTree v2.1.10 and visualized using iTOL.

Genome Comparison and Visualization

The BLAST Ring Image Generator (BRIG) was used to compare the PAO1 genome with the CAP *P. aeruginosa* genomes and to generate circular maps. Whole-genome alignments and synteny among the CAP genomes were assessed using Mauve.[17] Orthologous gene clustering was performed using OrthoFinder v2.4.0 with protein sequences from 87 genomes (3 CAP and 84 HAP) and default parameters.[18] Downstream analyses and figure generation were performed in R v4.3.2.

Ethics Statement

The study protocol was approved by the Ethical Review Committee of Peking University People's Hospital (Approval No. 2016PHB202-01) and registered at ClinicalTrials.gov (NCT03093220). This study was conducted in accordance with the Declaration of Helsinki (as revised in 2013). Written informed consent was obtained from all patients for study participation and for publication of their clinical case details and accompanying radiological images. All images were appropriately de-identified and contained no information that could identify individual patients.

Results

Case Presentation

To provide clinical context for the three CAP isolates subjected to whole-genome sequencing, we summarize three cases of severe CAP caused by *P. aeruginosa*, highlighting disease severity, radiographic phenotype, treatment course, and outcomes in relation to antimicrobial susceptibility.

Patient 1 (PARM801)

A 64-year-old woman was admitted on January 20, 2016, with an 18-day history of intermittent fever, cough, and sputum production. After transient symptom relief with outpatient medications, she developed recurrent fever with chills and a productive cough with greenish purulent sputum occasionally streaked with blood. She was a former smoker (5 pack-years; quit 8 years prior). Laboratory testing showed CRP 215 mg/L, neutrophils 15.7 × 10^9/L, and WBC 17.7 × 10^9/L. Sputum and blood cultures grew *P. aeruginosa* (PARM801), which was susceptible to most commonly used antipseudomonal agents (Table 1). Chest computed tomography (CT) demonstrated extensive consolidation and patchy opacities in the left upper lobe with left pleural effusion (Figure 1Ai). She received cefoperazone/sulbactam without clinical improvement and was switched to imipenem/cilastatin, after which fever and inflammatory markers improved (CRP 66.8 mg/L; neutrophils 7.4 × 10^9/L; WBC 9.3 × 10^9/L). Antibiotics were subsequently adjusted to ciprofloxacin plus ceftazidime, and she became afebrile within 3 days. Follow-up CT showed partial resolution of consolidation with minor internal cavitation and slightly reduced pleural effusion (Figure 1Aii). She was discharged on February 1 after clinical stabilization.

Patient 2 (PARM_L1)

A 61-year-old man was admitted on July 25, 2022, with 5 days of intermittent fever, accompanied by dyspnea, cough, and sputum production. He was a former smoker (25 pack-years; quit 2 years prior) with an 8-year history of chronic obstructive pulmonary disease and intermittent inhaled budesonide/formoterol use. On admission, he had mild cyanosis and moist rales over the left lung. Laboratory testing showed CRP 360.3 mg/L, absolute neutrophils 37.37 × 10^9/L, WBC 39.69 × 10^9/L, and albumin 25.4 g/L. Arterial blood gas analysis showed pH 7.374, $PaCO_2$ 42.9 mmHg, PaO_2 73.9 mmHg, and lactate 3.25 mmol/L. Chest CT revealed bilateral opacities with patchy high-density shadows in the left lung and localized cavitary lesions (Figure 1Bi). He was diagnosed with severe pneumonia complicated by sepsis and type I respiratory failure. BALF culture and blood next-generation sequencing detected *P. aeruginosa* (PARM_L1), which was susceptible to most antibiotics (Table 1). Empirical cefoperazone/sulbactam was initiated and then switched to meropenem due to persistent fever. Although inflammatory markers decreased, fever persisted, and repeat CT demonstrated radiographic progression with increased cavitation (Figure 1Bii). Treatment was escalated sequentially (piperacillin/tazobactam plus polymyxin B, followed by imipenem plus polymyxin B), but clinical and radiographic deterioration continued. The patient chose voluntary discharge on August 7 for further treatment at another hospital.

Patient 3 (PARM_Z1)

A 59-year-old man presented on July 31, 2022, with 2 days of fever and cough and 9 hours of chest pain. He reported rusty sputum and had a 50-pack-year smoking history and long-term alcohol consumption. Initial treatment at a local

Table 1 MICs of the 3 Clinically Isolated CAP *P. aeruginosa* Strains Against Common Antimicrobial Agents

Antimicrobial agents	MIC (mg/L)/Antimicrobial Susceptibility		
	PARM801	PARM_L1	PARM_Z1
Piperacillin/tazobactam	<=4/S	<=4/S	8/S
Tobramycin	<=1/S	<=1/S	<=1/S
Ticarcillin/clavulanate	–	16/S	16/S
Ceftazidime	<=1/S	2/S	2/S
Cefoperazone/sulbactam	<=8/S	<=8/S	<=8/S
Meropenem	0.5/S	<=0.25/S	<=0.25/S
Levofloxacin	0.5/S	0.5/S	1/S
Imipenem	2/S	2/S	2/S
Cefepime	<=1/S	2/S	2/S
Polymyxin B	2/I	<=0.5/I	2/I
Ciprofloxacin	<=0.25/S	<=0.25/S	<=0.25/S
Amikacin	<=2/S	<=2/S	<=2/S

Abbreviations: S, susceptible; I, intermediate; –, not tested.

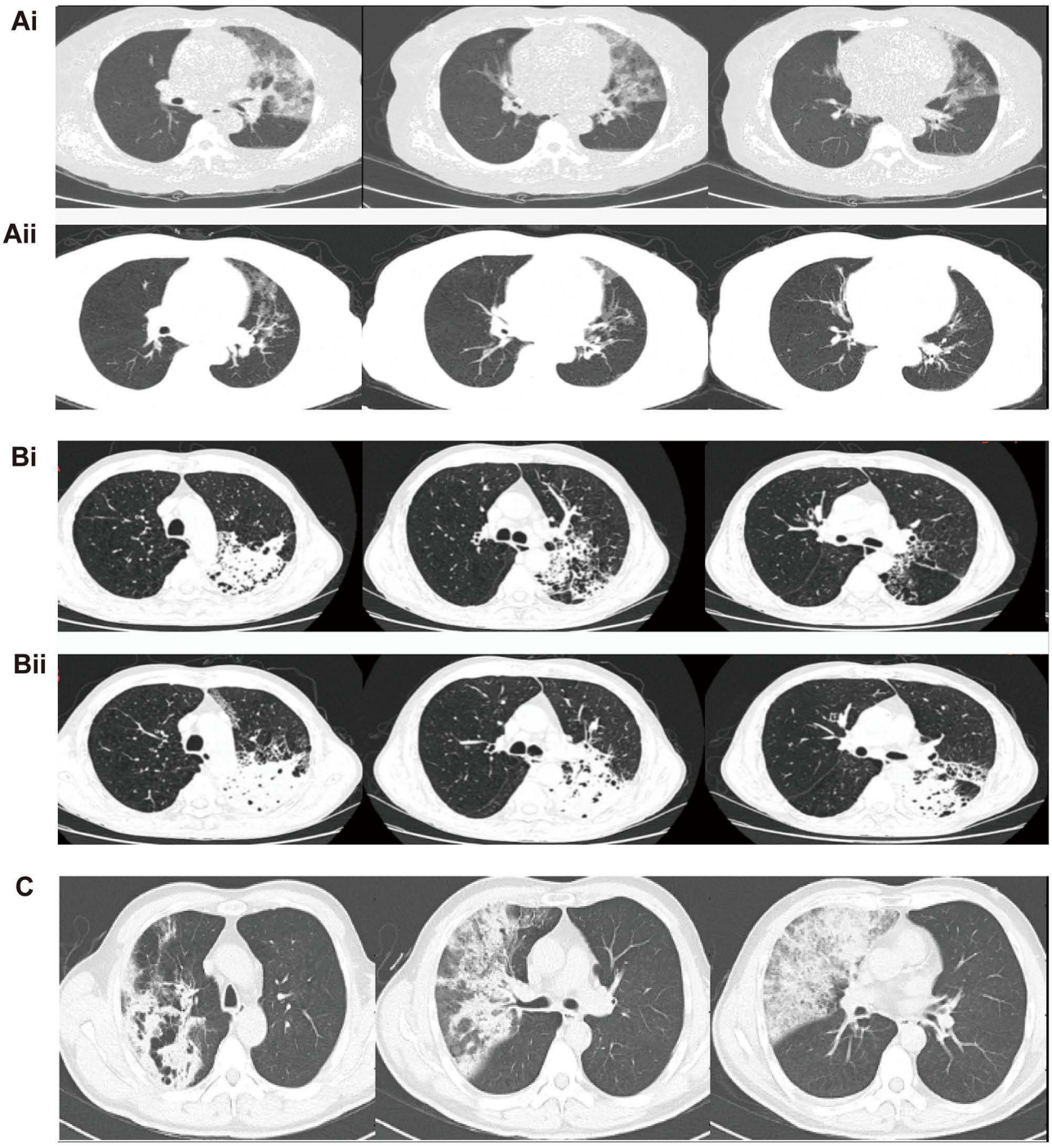

Figure 1 Chest computed tomography of three patients on admission and after admission. (**Ai**) Chest CT of patient 1 on admission showed large areas of consolidation and patchy blurry shadows in the upper lobe of the left lung, with scattered dense shadows in the bilateral lung and left pleural effusion. (**Aii**) On the 25th day after admission, a repeat CT of patient 1 showed the left upper lobe infection was further absorbed and localized than before, with minor internal cavity shadows before the patient was discharged in improved condition. (**Bi**) The chest CT of patient 2 on admission showed increased opacity in both lungs, patchy high-density shadows in the left lung, bronchial shadows seen inside, and local cavity shadows visible. (**Bii**) Repeat CT of patient 2 on Day 6 was more rapidly progressive with clinical deterioration than before and found local cavity formation. (**C**) Chest CT of patient 3 on admission showed patchy high-density shadows in the upper and middle lobes of the right lung with a small amount of pleural effusion.

clinic did not improve symptoms. On admission, CRP was 276.6 mg/L, WBC 13.47 × 10^9/L, neutrophils 90.1%, serum creatinine 192.1 μmol/L, and total protein 59.3 g/L. Arterial blood gas analysis showed pH 7.40, $PaCO_2$ 30.3 mmHg, PaO_2 91.14 mmHg, and lactate 1.55 mmol/L. Chest CT showed patchy consolidation in the right upper and middle lobes with a small pleural effusion (Figure 1C). BALF culture yielded *P. aeruginosa* (PARM_Z1), which was susceptible to

https://doi.org/10.2147/IDR.S566637

commonly used antipseudomonal agents (Table 1). Despite piperacillin/tazobactam therapy, he rapidly deteriorated with worsening hemoptysis, dyspnea, and chest pain, requiring intensive care unit (ICU) admission and mechanical ventilation. Antibiotics were escalated to piperacillin/tazobactam plus moxifloxacin; however, he developed septic shock and cardiac arrest. Repeat arterial blood gas analysis showed severe respiratory acidosis and hypoxemia (pH 7.04, $PaCO_2$ 142.6 mmHg, PaO_2 27.39 mmHg) with hyperkalemia, hypoglycemia, and elevated lactate (7.76 mmol/L). Resuscitation was unsuccessful, and he died on August 1.

The three CAP cases had an acute onset and severe clinical course, characterized by marked systemic inflammation (elevated CRP and neutrophilia). Two patients exhibited lobar consolidation with cavitation and progressed to sepsis or septic shock, resulting in one fatality. Strikingly, despite the clinical severity, all three CAP isolates remained broadly susceptible to standard antipseudomonal agents in vitro (Table 1). This distinct clinical phenotype prompted a comparative genomic analysis to determine how CAP isolates differ from HAP-associated genomes regarding antimicrobial resistance determinants, virulence gene content, and CAP-specific genes contributing to niche adaptation and pathogenic potential.

Genomic Characteristics

The genomic features of the three fully sequenced CAP *P. aeruginosa* strains are summarized in Table 2. Each genome consisted of a single circular chromosome and no plasmids were detected. The assembled genome sizes of the CAP *P. aeruginosa* strains range from 6.5 to 7.1 Mb, exceeding the 6.3 Mb genome of PAO1, with a GC content varying from 65.76% to 66.41%. The CAP *P. aeruginosa* genome is slightly larger than that of PAO1 (6.3 Mb). The predicted numbers of protein-coding sequences (CDSs) ranged from 5908 to 6633. All three genomes contained 12 rRNA genes and 65 tRNA genes.

MLST analysis assigned PARM801 and PARM_L1 to ST2475 and ST205, respectively, whereas PARM_Z1 was identified as a novel sequence type. The BRIG comparison against PAO1 indicated that the three CAP genomes shared a largely conserved genomic backbone with the reference, showing extensive high-identity alignments across most of the chromosome and only discrete low-identity or absent segments (Figure 2A). Whole-genome alignment further demonstrated extensive synteny among the three CAP genomes relative to PAO1, with most loci residing within shared locally collinear blocks (LCBs); several rearrangements (including inversions and translocations among blocks) were observed across strains (Figure 2B).

Phylogenetic and Comparative Genomic Analysis

To investigate the genetic relationships among *P. aeruginosa* pneumonia strains, we constructed ML trees using core genome SNPs from three CAP strains and 84 HAP strains retrieved from the RefSeq database. Phylogenetic analysis based on core SNPs revealed that all 87 isolates clustered into three distinct clades (Figure 3). Notably, all the CAP strains were grouped within the same clade, suggesting a close genetic relationship. Additionally, MLST identified 50 distinct STs among the 87 *P. aeruginosa* isolates. The most prevalent STs were ST395 (9.2%, n = 8), ST253 (8.0%, n = 7), and ST1971 (8.0%, n = 7), followed by ST235 (4.6%, n = 4), ST309 (4.6%, n = 4), and ST357 (4.6%, n = 4). These findings demonstrate significant genetic heterogeneity among the isolates, with distinct clustering patterns observed for the CAP and HAP strains.

Distribution of Antibiotic-Resistant Determinants

Although the drug sensitivity results for all CAP *P. aeruginosa* strains in this study showed sensitivity to almost all common antibiotics, given the clinical importance of AMR in *P. aeruginosa*, we compared the distributions of AMR

Table 2 Genome Features of the 3 Completely Sequenced CAP *P. aeruginosa* Strains

Strains	Genetic Material	Size (bp)	GC Content%	Gene	rRNA	tRNA
PARM_L1	Chromosome	6468200	66.41	5908	12	65
PARM_Z1	Chromosome	6566704	66.31	5989	12	65
PARM801	Chromosome	7130567	65.76	6633	12	65

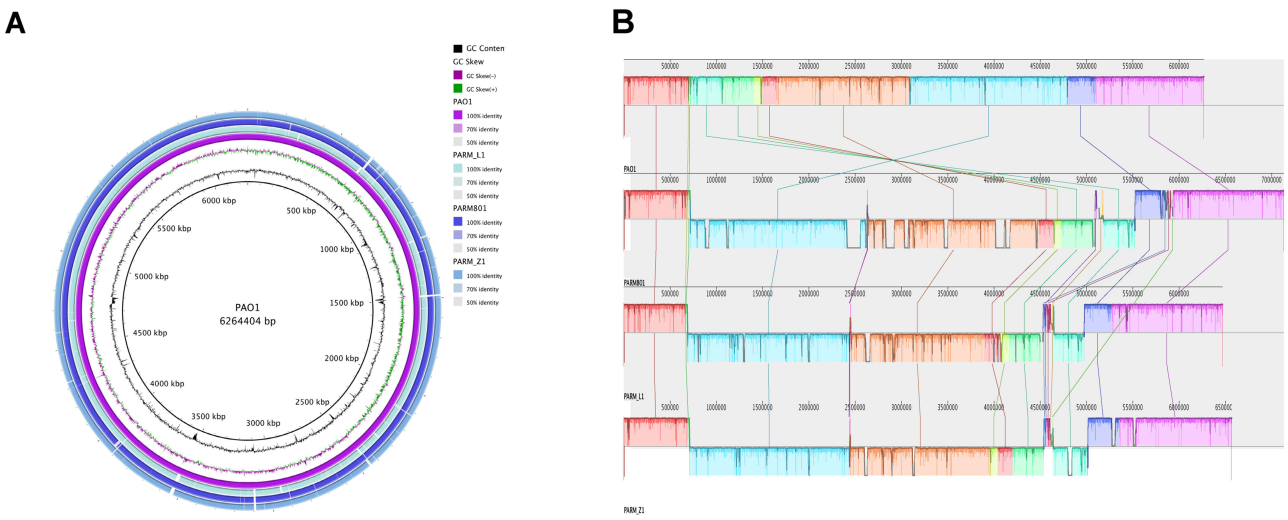

Figure 2 (**A**) The BLAST Ring Image Generator (BRIG) circular comparison of PARM_L1, PARM_Z1, and PARM801 mapped to the PAO1 chromosome. Concentric rings represent BLAST alignments of each CAP genome to PAO1. Shading reflects nucleotide identity according to BRIG bins; unshaded regions indicate no detectable alignment to PAO1 under the specified parameters. (**B**) Whole-genome synteny of PARM_L1, PARM_Z1, and PARM801 relative to PAO1 assessed by Mauve. Colored blocks denote locally collinear blocks (LCBs), and connecting lines trace homologous LCBs across genomes; block order and orientation differences indicate rearrangements.

determinants in the three CAP genomes with those in the 84 publicly available HAP genomes. The antimicrobial resistance genes across the 87 genomes are shown in Figure 4. Among aminoglycoside-associated determinants, *aph(3')-IIb, emrE*, and *soxR* were detected in all genomes (CAP 3/3; HAP 84/84), indicating conservation across groups (Figure 4), whereas other aminoglycoside-resistant genes were entirely conserved in the HAP group but absent in the CAP group. The *armR* gene was strictly conserved in all analyzed genomes, and $bla_{\text{PDC-6}}$ was specifically conserved in all CAP strains. Additionally, β-lactamases $bla_{\text{OXA-486}}$, $bla_{\text{OXA-50}}$, $bla_{\text{PDC-5}}$, and $bla_{\text{PDC-7}}$ were detected in the CAP group. However, several β-lactamases, such as OXA-type, PDC-type, and TEM-type variants, were more frequently detected in the HAP group. For fosfomycin-associated loci, *fosA, arnA*, and *basS* were detected in all genomes (CAP 3/3; HAP 84/84). Furthermore, the fluoroquinolone resistance gene *crpP* was detected in all CAP strains (3/3).

Resistance-associated mutations were detected in both CAP and HAP isolates, but the mutational spectra differed between groups (HAP, n = 84; CAP, n = 3), as shown in Figure 4. No quinolone resistance-determining region (QRDR) substitutions in *gyrA, parC* and *parE* were identified in CAP isolates (0/3). In contrast, multiple QRDR variants were observed in HAP isolates, including *gyrA*(D87N) (1/84), *gyrA*(D87G) (1/84), *gyrA*(T83I) (23/84), *parC*(S87L) (19/84), *parC*(S87W) (1/84), and *parE*(A473V) (2/84). Several β-lactam–associated alterations were restricted to HAP isolates, including *ampD*(A134V) (8/84), *ampD*(A136V) (3/84), *ampD*(Q44H) (11/84), *dacB*(V289I) (1/84), and *ftsI*(A504C) (1/84). *nalC* variants were present in both groups, with G71E, S209R, and A186T detected in 78/84, 58/84, and 6/84 HAP isolates and in 2/3, 2/3, and 1/3 CAP isolates, respectively. Although all CAP isolates were categorized as intermediate to polymyxin B, *pmrA*(L71R) was detected in 2/3 CAP isolates (and 53/84 HAP isolates), indicating the presence of a polymyxin-associated regulatory variant despite retained susceptibility in our testing. Overall, HAP isolates harbored a broader diversity and higher frequency of resistance-associated mutations than CAP isolates.

Presence of Virulence Genes

To compare the pathogenic potential of isolates from the two groups, we profiled the presence/absence of curated *Pseudomonas* virulence genes across all genomes. In total, 439 virulence-associated genes were detected among the 87 genomes. Of these, 285/439 (64.88%) were assigned to key pathogenic processes, including biofilm formation, exoenzyme/toxin production, effector delivery systems, motility, nutritional/metabolic adaptation, adherence, and immune modulation (Supplementary Table 2). The overall distribution patterns were broadly similar between CAP and HAP isolates, indicating that the core virulence gene repertoire was largely conserved.

https://doi.org/10.2147/IDR.S566637

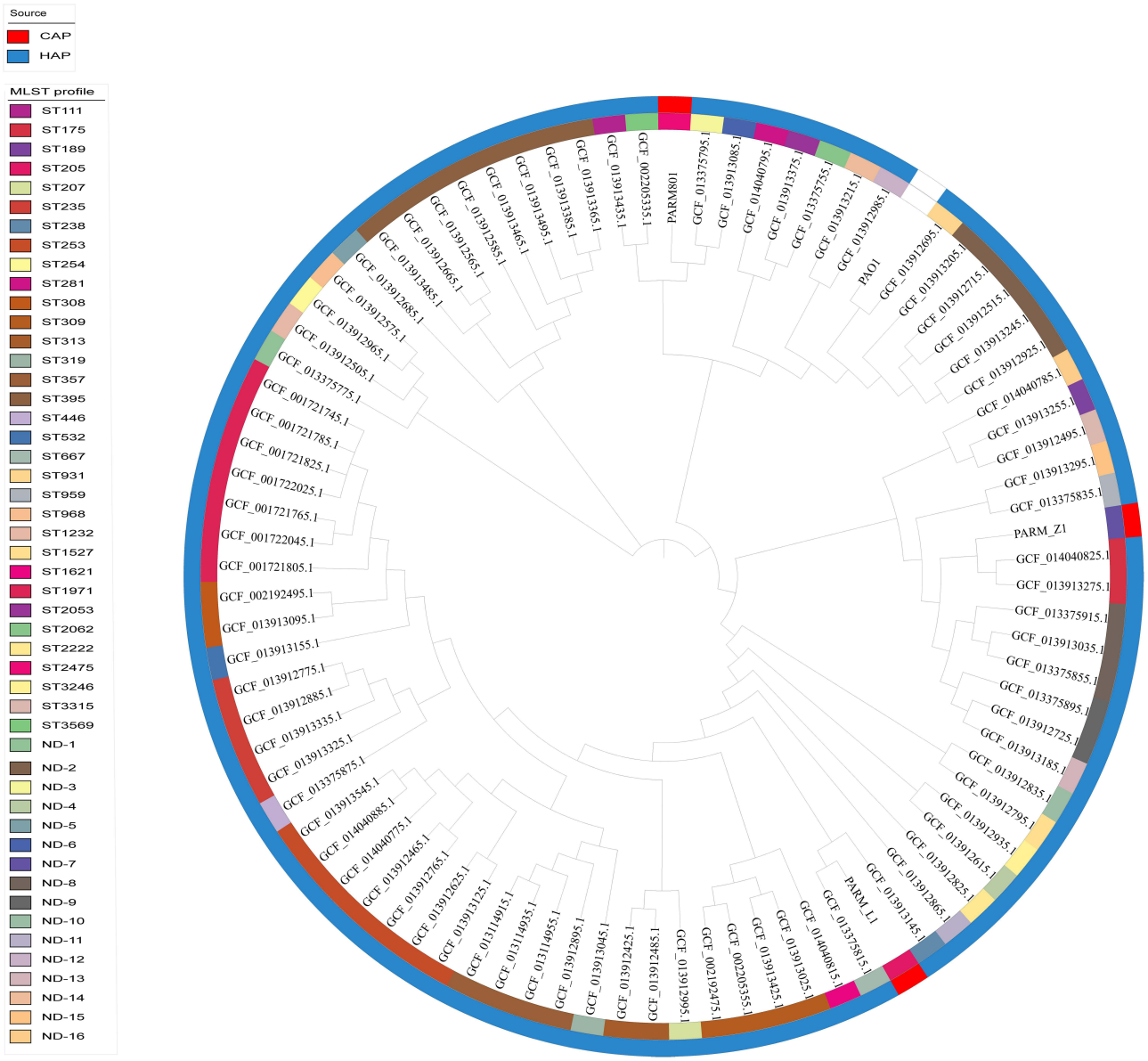

Figure 3 Core SNP phylogenetic tree of 84 *P. aeruginosa* genomes downloaded from NCBI RefSeq and the present study. Strain names of isolates belonging to the CAP are colored in red and HAP in blue. Outer ring strips are colored according to STs.

Further analysis of differentially distributed genes revealed that, compared with HAP isolates, the CAP group uniformly lacked 40 virulence genes (genes scored as 0 across all CAP genomes) (Figure 5 and Supplementary Table 3). These CAP-absent genes were mainly involved in immune modulation (33/40), biofilm formation (4/40), and effector delivery systems (3/40). The missing immune modulation–related genes included *asnB, hisF, hisH2, neuC, tviB, tviC, wecC*, as well as multiple locus-tagged genes (*PA14_RS09475–PA14_RS09500, PA14_RS29910–PA14_RS29920, PLES_RS09885 and PLES_RS09905–PLES_RS09940, PSPA7_RS09425, PSPA7_RS09460, PSPA7_RS30415, PSPA7_RS30430, PSPA7_RS30875, PSPA7_RS30880, PSPA7_RS31970, PSPA7_RS31975, and pseB*) (Figure 5 and Supplementary Table 3). In addition, four biofilm-associated genes (PA14_RS24355, PA14_RS24360, PA14_RS24370, PA14_RS24375) and three effector delivery system–associated genes, including the putative T6SS-associated effectors *pldA/tle5a* and *rhsP2*, and the T3SS chaperone *spcU* were not detected in the CAP isolates (Figure 5 and Supplementary Table 3). Among major T3SS effector genes, *exoU* was detected only in PARM_L1, whereas *exoS* was present in PARM801 and PARM_Z1; clinically, the PARM_L1 case showed persistent fever and radiographic progression with increasing cavitation prior to transfer despite sequential escalation of antipseudomonal therapy.

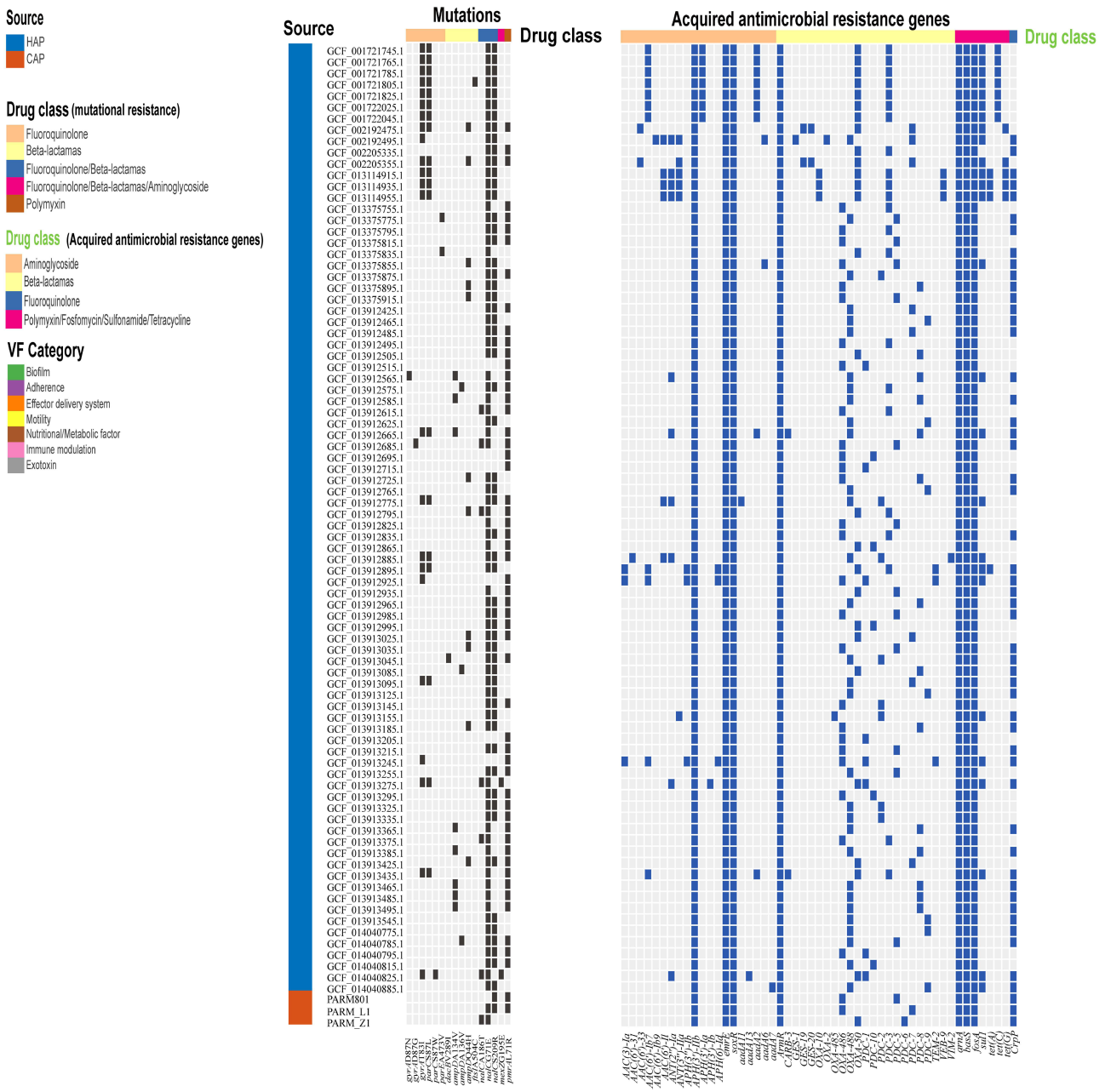

Figure 4 Distributions of resistance-associated mutations and acquired AMR genes. Squares, which are colored by trait category, represent the presence of the trait examined.

Specific Genes in CAP *P. aeruginosa* Strains

A total of 10,225 gene families (orthogroups) were identified across 87 genomes, comprising 4460 core gene families (present in all genomes; 43.6%), 5664 accessory gene families (present in 2–86 genomes; 55.4%), and 101 unique gene families (present in only one genome; 0.99%) (Figure 6A). At the group level, 6584 gene families were observed in at least one CAP genome, of which 6566 were shared with the HAP group and 18 were exclusive to CAP (Figure 6B). In addition to CAP-exclusive orthogroups (n=18), CAP-specific genes also included genes present in CAP genomes but not assigned to any orthogroup by OrthoFinder (unassigned), resulting in 157 CAP-specific genes in total (Supplementary Table 4). COG annotation showed that most CAP-specific genes were poorly characterized, including unclassified genes (n=120) and COG category S (function unknown, n=7), totaling 127; the next most common category was lipid transport

https://doi.org/10.2147/IDR.S566637

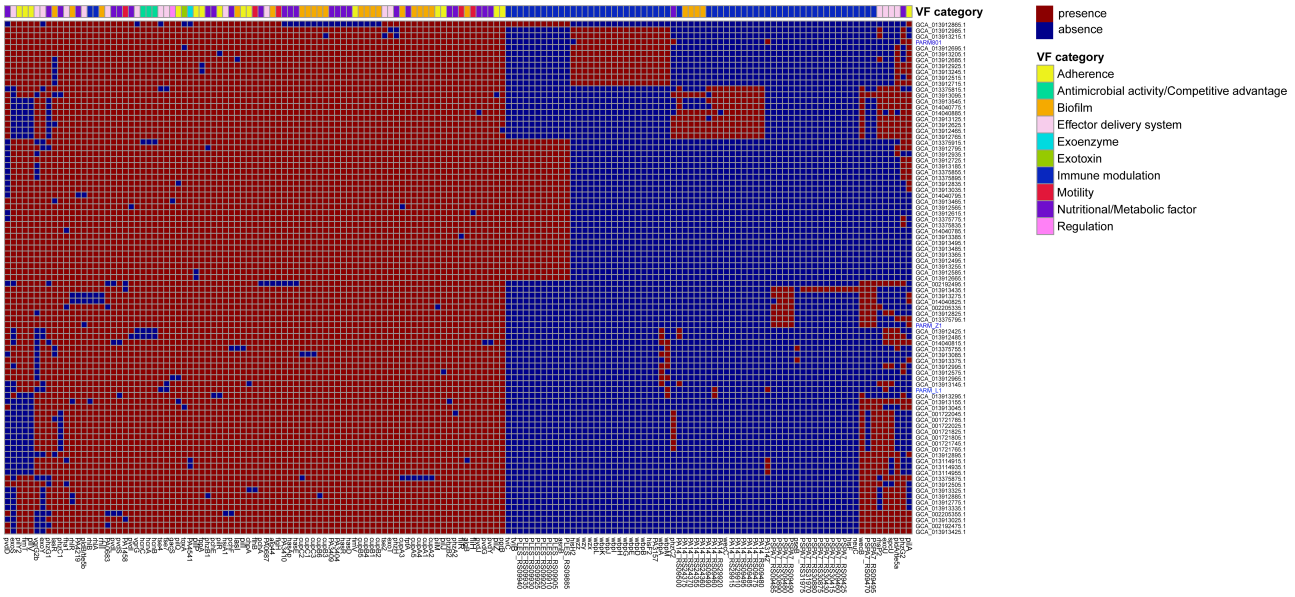

Figure 5 Distribution of non-conserved virulence genes. Squares, colored by trait category, indicate the presence of the examined trait. The three CAP samples are marked in blue font.

and metabolism (I, n=11) (Figure 6C). These include *paaF, fadL, HIBADH* (3-hydroxyisobutyrate dehydrogenase), enoyl-CoA hydratase/isomerase family proteins, SDR family oxidoreductases, and 3-hydroxyacyl-CoA dehydrogenases.

Discussion

In this study, we integrated detailed clinical phenotyping of three severe CAP cases caused by *P. aeruginosa* with a comparative genomic analysis of 84 complete HAP-associated genomes. Clinically, all three cases manifested with abrupt onset, marked systemic inflammation, and extensive radiographic consolidation accompanied by cavitation or pleural effusion. Notably, two patients progressed to sepsis or septic shock, resulting in one fatality. This severe phenotype aligns with prior reports indicating that *P. aeruginosa* CAP, though uncommon, follows a fulminant course associated with substantial mortality, even in immunocompetent hosts.[19–21] While recent reviews estimate that *P. aeruginosa* constitutes a minority of culture-positive CAP cases (4%), it carries a disproportionately high fatality rate (33–66%), particularly when necrotizing or hemorrhagic patterns are present.[22] However, the precise mechanisms driving the progression from such severe CAP to septic shock and multiple organ dysfunction syndrome (MODS) remain to be fully elucidated.

Remarkably, despite the fulminant disease course, all CAP isolates in our cohort remained broadly susceptible to antipseudomonal agents in vitro. This observation aligns with epidemiologic data suggesting that community-acquired *P. aeruginosa* typically displays a non-multidrug-resistant (MDR) phenotype compared to nosocomial strains. In a prospective cohort, *P. aeruginosa* accounted for 4% of CAP cases, yet only 32% of these were MDR.[23] In contrast, HAP surveillance in Asia reports significantly higher rates of MDR (42.8%), reflecting the sustained antibiotic and device-associated selective pressures inherent to hospital ecosystems.[24] Concordantly, our genomic comparisons showed that the CAP isolates carried fewer acquired AMR determinants and fewer canonical resistance-associated mutations than HAP genomes, supporting the ecological model that community strains face less continuous antimicrobial selection, while hospital-adapted populations accumulate resistance determinants under repeated exposure.

Beyond antimicrobial resistance, our virulence profiling showed that the CAP isolates consistently lacked a subset of virulence-associated genes present in the HAP reference set, most of which were labeled as immune modulation. However, this pattern may not be interpreted as reduced virulence. A substantial fraction of these hits map to highly variable surface polysaccharide loci, including the O-antigen biosynthetic region, a well-recognized hotspot of serotype-dependent diversification. Accordingly, the absence of these HAP-associated markers in CAP isolates may

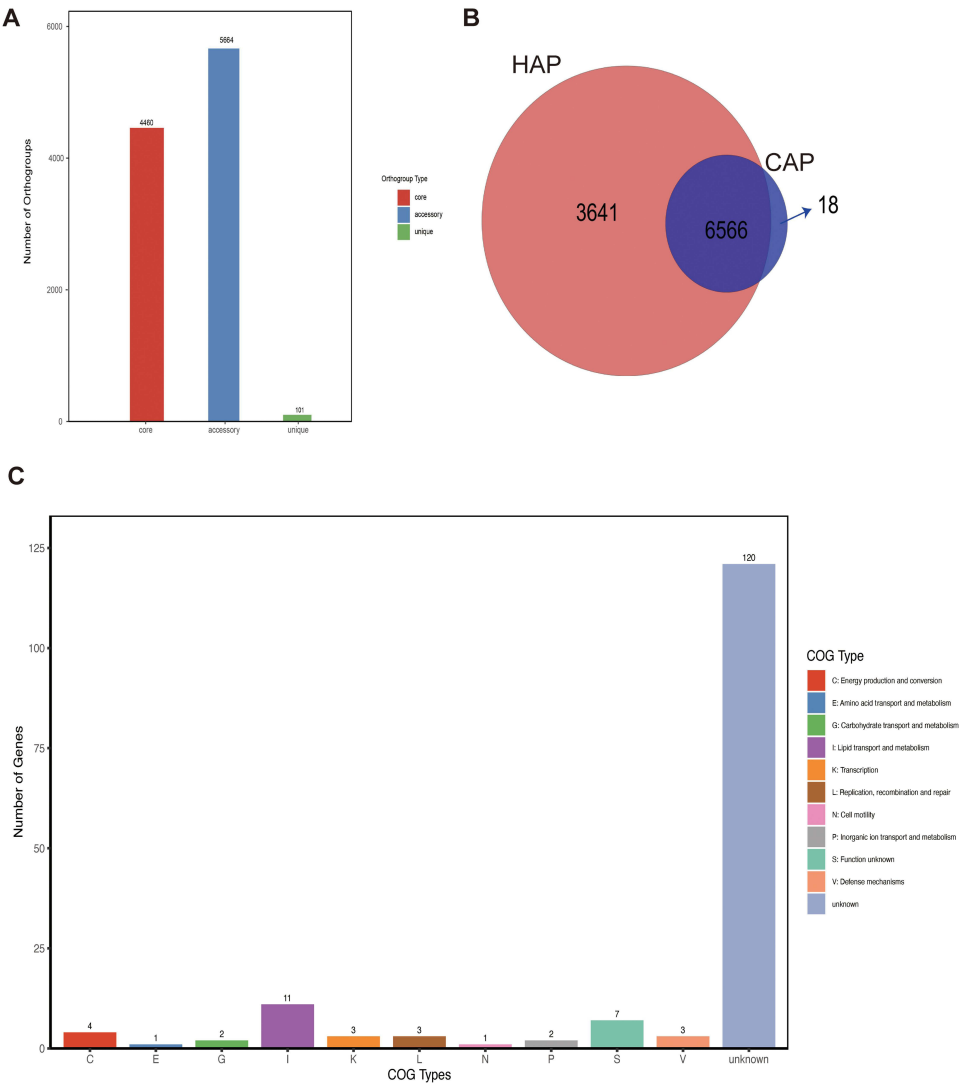

Figure 6 Pangenome summary and functional annotation of CAP-specific genes. (**A**) Bar chart showing the statistics of gene families. (**B**) Venn diagram illustrating the overlap of gene families between CAP (blue) and HAP groups (red). (**C**) Bar chart of COG annotation statistics for CAP-specific genes, showing their functional classification.

reflect serotype differences rather than a true loss of immune-evasion capacity.[25] Consistent with this, our clinical genomic integration highlights that severe CAP can be driven by high-impact determinants rather than by a higher overall count of virulence genes. Notably, the T3SS effector ExoU was detected in PARM_L1 (Patient 2), which was characterized by persistent fever and radiographic progression with increasing cavitation despite sequential escalation of antipseudomonal therapy, consistent with experimental evidence that ExoU-mediated cytotoxicity contributes to severe lung injury and early pneumonia severity.[26,27] Meanwhile, *exoS* was present in PARM801 and PARM_Z1 (including the fatal case), supporting the concept that distinct T3SS effector repertoires may underlie severe disease via different mechanisms; ExoS has been shown to disrupt the pulmonary vascular barrier and facilitate dissemination during pneumonia in vivo.[28]

Our pangenome analysis identified 157 genes unique to the CAP cohort, with a notable subset annotated to lipid transport and metabolism. This functional pattern is mechanistically plausible because pulmonary surfactant is rich in lipids, with phosphatidylcholine representing a major fraction of surfactant lipids.[29,30] Consistent with this niche pressure, *P. aeruginosa* can degrade components of pulmonary surfactant in vitro, potentially reshaping the local availability of lipid substrates during infection.[31] Importantly, exposure to exogenous fatty acids can remodel *P. aeruginosa* membrane phospholipid composition, alter membrane permeability, and shift virulence-associated

https://doi.org/10.2147/IDR.S566637

phenotypes, supporting a link between environmental fatty acids and clinically relevant behaviors.[32] Regulatory and in vivo evidence further connects long-chain fatty acid utilization to pathogenesis. In our dataset, CAP-specific genes included lipid-associated functions, such as *fadL* and multiple enzymes in acyl-CoA and fatty-acid–associated metabolism. Prior studies show that the LCFA-responsive regulator *PsrA* is linked to induction of fatty-acid degradation functions during lung infection, and that *PvrA* contributes to pathogenesis by controlling bacterial utilization of long-chain fatty acids.[33,34] FadL-family outer membrane proteins also participate in fatty-acid handling and stress-adaptive physiology, and the FadL homolog ExFadLO has been characterized as an outer membrane transporter required for exporting oxygenated LCFA derivatives.[35] Collectively, these data support the interpretation that the CAP-specific gene subset involved in lipid utilization and lipid handling may enhance fitness in an inflamed airway environment that is rich in surfactant lipids and fatty acids, potentially contributing to persistence and tissue injury.

Our study is subject to several limitations. First, the small sample size of the CAP cohort (n=3), reflecting the clinical rarity of this condition, limits statistical power; consequently, our comparisons between CAP and HAP should be interpreted as descriptive and hypothesis-generating rather than definitive. Second, the HAP comparison group was restricted to complete RefSeq assemblies, which may introduce selection bias toward specific lineages or historical surveillance priorities. Future work should expand CAP sampling across regions and years, incorporate contemporaneous geographically matched HAP isolates, and pair comparative genomics with functional assays. Priority validation experiments include assessing bacterial growth and transcriptional responses in conditions supplemented with pulmonary surfactant or fatty acids and characterizing membrane lipid composition and permeability after exposure to exogenous fatty acids.

Conclusion

We sequenced three *P. aeruginosa* isolates from CAP and compared them with 84 complete HAP associated genomes. Despite severe disease with sepsis or septic shock and one death, the CAP isolates remained broadly susceptible in vitro and showed a lower burden of acquired antimicrobial resistance genes and fewer resistance associated variants than the HAP. Severe disease may be associated with the T3SS effector profile (*exoU* or *exoS*) and with CAP-specific accessory genes, including genes involved in lipid transport and metabolism that may support adaptation to the airway environment and membrane remodeling under inflammatory stress. Given the small number of CAP isolates, these comparisons are descriptive and require validation in larger cohorts and functional studies.

Data Sharing Statement

The datasets supporting this study are publicly available in the GenBank nucleotide database under accession numbers CP135174, CP135175, and CP024024.

Funding

This work was supported by grants from the National Natural Science Foundation of China [grant numbers 81870010 and 81903672] and National and Provincial Key Clinical Specialty Capacity Building Project 2020.

Disclosure

The authors declare that this research was conducted in the absence of any commercial or financial relationships that could be construed as potential conflicts of interest.

References

1. Reynolds D, Kollef M. The epidemiology and pathogenesis and treatment of pseudomonas aeruginosa infections: an update. *Drugs*. 2021;81(18):2117–2131. doi:10.1007/s40265-021-01635-6
2. Maharaj S, Isache C, Seegobin K, Chang S, Nelson G. Necrotizing pseudomonas aeruginosa community-acquired pneumonia: a case report and review of the literature. *Case Rep Infect Dis*. 2017;2017:1717492. doi:10.1155/2017/1717492
3. Klockgether J, Cramer N, Wiehlmann L, Davenport CF, Tümmler B. Pseudomonas aeruginosa genomic structure and diversity. *Front Microbiol*. 2011;2:150. doi:10.3389/fmicb.2011.00150
4. Hwang W, Yong JH, Min KB, et al. Genome-wide association study of signature genetic alterations among pseudomonas aeruginosa cystic fibrosis isolates. *PLoS Pathog*. 2021;17(6):e1009681. doi:10.1371/journal.ppat.1009681

5. Kung VL, Ozer EA, Hauser AR. The accessory genome of Pseudomonas aeruginosa. *Microbiol Mol Biol Rev*. 2010;74(4):621–641. doi:10.1128/MMBR.00027-10
6. Subedi D, Kohli GS, Vijay AK, Willcox M, Rice SA. Accessory genome of the multi-drug resistant ocular isolate of Pseudomonas aeruginosa PA34. *PLoS One*. 2019;14(4):e0215038. doi:10.1371/journal.pone.0215038
7. Dettman JR, Kassen R. Evolutionary genomics of niche-specific adaptation to the cystic fibrosis lung in Pseudomonas aeruginosa. *Mol Biol Evol*. 2021;38(2):663–675. doi:10.1093/molbev/msaa226
8. Livermore DM. Multiple mechanisms of antimicrobial resistance in Pseudomonas aeruginosa: our worst nightmare? *Clin Infect Dis*. 2002;34(5):634–640. doi:10.1086/338782
9. Del Barrio-Tofiño E, López-Causapé C, Cabot G, et al. Genomics and susceptibility profiles of extensively drug-resistant Pseudomonas aeruginosa isolates from Spain. *Antimicrob Agents Chemother*. 2017;61(11). doi:10.1128/aac.01589-17
10. Roy Chowdhury P, Scott MJ, Djordjevic SP. Genomic islands 1 and 2 carry multiple antibiotic resistance genes in Pseudomonas aeruginosa ST235, ST253, ST111 and ST175 and are globally dispersed. *J Antimicrob Chemother*. 2017;72(2):620–622. doi:10.1093/jac/dkw471
11. Liao C, Huang X, Wang Q, Yao D, Lu W. Virulence factors of pseudomonas aeruginosa and antivirulence strategies to combat its drug resistance. *Front Cell Infect Microbiol*. 2022;12:926758. doi:10.3389/fcimb.2022.926758
12. Koren S, Walenz BP, Berlin K, Miller JR, Bergman NH, Phillippy AM. Canu: scalable and accurate long-read assembly via adaptive k-mer weighting and repeat separation. *Genome Res*. 2017;27(5):722–736. doi:10.1101/gr.215087.116
13. Seemann T. Prokka: rapid prokaryotic genome annotation. *Bioinformatics*. 2014;30(14):2068–2069. doi:10.1093/bioinformatics/btu153
14. Jia B, Raphenya AR, Alcock B, et al. CARD 2017: expansion and model-centric curation of the comprehensive antibiotic resistance database. *Nucleic Acids Res*. 2017;45(D1):D566–d573. doi:10.1093/nar/gkw1004
15. Chen L, Zheng D, Liu B, Yang J, Jin Q. VFDB 2016: hierarchical and refined dataset for big data analysis--10 years on. *Nucleic Acids Res*. 2016;44(D1):D694–7. doi:10.1093/nar/gkv1239
16. Del Barrio-Tofiño E, Zamorano L, Cortes-Lara S, et al. Spanish nationwide survey on Pseudomonas aeruginosa antimicrobial resistance mechanisms and epidemiology. *J Antimicrob Chemother*. 2019;74(7):1825–1835. doi:10.1093/jac/dkz147
17. Darling AC, Mau B, Blattner FR, Perna NT. Mauve: multiple alignment of conserved genomic sequence with rearrangements. *Genome Res*. 2004;14(7):1394–1403. doi:10.1101/gr.2289704
18. Emms DM, Kelly S. OrthoFinder: phylogenetic orthology inference for comparative genomics. *Genome Biol*. 2019;20(1):238. doi:10.1186/s13059-019-1832-y
19. Rahdar HA, Kazemian H, Bimanand L, et al. Community acquired pseudomonas aeruginosa Pneumonia in a young athlete man: a case report and literature review. *Infect Disord Drug Targets*. 2018;18(3):249–254. doi:10.2174/1871526518666180410122531
20. Wang T, Hou Y, Wang R. A case report of community-acquired Pseudomonas aeruginosa pneumonia complicated with MODS in a previously healthy patient and related literature review. *BMC Infect Dis*. 2019;19(1):130. doi:10.1186/s12879-019-3765-1
21. Wang J, Yun L, Zhao H, Li X. Combination therapy of polymyxin B and amikacin for community-acquired Pseudomonas aeruginosa Pneumonia with MODS in a previously healthy patient: a case report. *Infect Drug Resist*. 2021;14:2895–2900. doi:10.2147/IDR.S312601
22. Barp N, Marcacci M, Biagioni E, et al. A fatal case of Pseudomonas aeruginosa community-acquired pneumonia in an immunocompetent patient: clinical and molecular characterization and literature review. *Microorganisms*. 2023;11(5):1112. doi:10.3390/microorganisms11051112
23. Cilloniz C, Gabarrus A, Ferrer M, et al. Community-acquired pneumonia due to multidrug- and non-multidrug-resistant Pseudomonas aeruginosa. *Chest*. 2016;150(2):415–425. doi:10.1016/j.chest.2016.03.042
24. Chung DR, Song JH, Kim SH, et al. High prevalence of multidrug-resistant nonfermenters in hospital-acquired pneumonia in Asia. *Am J Respir Crit Care Med*. 2011;184(12):1409–1417. doi:10.1164/rccm.201102-0349OC
25. Raymond CK, Sims EH, Kas A, et al. Genetic variation at the O-antigen biosynthetic locus in Pseudomonas aeruginosa. *J Bacteriol*. 2002;184(13):3614–3622. doi:10.1128/JB.184.13.3614-3622.2002
26. Howell HA, Logan LK, Hauser AR. Type III secretion of ExoU is critical during early Pseudomonas aeruginosa pneumonia. *mBio*. 2013;4(2):e00032–13. doi:10.1128/mBio.00032-13
27. Schulert GS, Feltman H, Rabin SD, et al. Secretion of the toxin ExoU is a marker for highly virulent Pseudomonas aeruginosa isolates obtained from patients with hospital-acquired pneumonia. *J Infect Dis*. 2003;188(11):1695–1706. doi:10.1086/379372
28. Rangel SM, Diaz MH, Knoten CA, Zhang A, Hauser AR. The role of ExoS in dissemination of Pseudomonas aeruginosa during Pneumonia. *PLoS Pathog*. 2015;11(6):e1004945. doi:10.1371/journal.ppat.1004945
29. Han S, Mallampalli RK. The Role of Surfactant in Lung Disease and Host Defense against Pulmonary Infections. *Ann Am Thorac Soc*. 2015;12(5):765–774. doi:10.1513/AnnalsATS.201411-507FR
30. Veldhuizen R, Nag K, Orgeig S, Possmayer F. The role of lipids in pulmonary surfactant. *Biochim Biophys Acta*. 1998;1408(2–3):90–108. doi:10.1016/s0925-4439(98)00061-1
31. Beatty AL, Malloy JL, Wright JR. Pseudomonas aeruginosa degrades pulmonary surfactant and increases conversion in vitro. *Am J Respir Cell Mol Biol*. 2005;32(2):128–134. doi:10.1165/rcmb.2004-0276OC
32. Baker LY, Hobby CR, Siv AW, et al. Pseudomonas aeruginosa responds to exogenous polyunsaturated fatty acids (PUFAs) by modifying phospholipid composition, membrane permeability, and phenotypes associated with virulence. *BMC Microbiol*. 2018;18(1):117. doi:10.1186/s12866-018-1259-8
33. Pan X, Fan Z, Chen L, et al. PvrA is a novel regulator that contributes to Pseudomonas aeruginosa pathogenesis by controlling bacterial utilization of long chain fatty acids. *Nucleic Acids Res*. 2020;48(11):5967–5985. doi:10.1093/nar/gkaa377
34. Kang Y, Nguyen DT, Son MS, Hoang TT. The Pseudomonas aeruginosa PsrA responds to long-chain fatty acid signals to regulate the fadBA5 beta-oxidation operon. *Microbiology*. 2008;154(Pt 6):1584–1598. doi:10.1099/mic.0.2008/018135-0
35. Martinez E, Estupinan M, Pastor FI, Busquets M, Diaz P, Manresa A. Functional characterization of ExFadLO, an outer membrane protein required for exporting oxygenated long-chain fatty acids in Pseudomonas aeruginosa. *Biochimie*. 2013;95(2):290–298. doi:10.1016/j.biochi.2012.09.032